Pesquisas em Geociências
GEOCIÊNCIAS
v. 51, nº 1 (2024)
doi.org/10.22456/1807-9806.137321

Research Article

Brittleness Index Application on a Jurassic Mudstone Source Rock Interval, Case Study: Poseidon 2 well, Browse Basin, Australia

Aplicação do Índice de Fragilidade em um intervalo de rocha geradora de lutito do Jurássico, Estudo de caso: Poço Poseidon 2, Bacia Browse, Austrália

Kristhian Leandro PEÑA CERÓN[1], *Sugeng Sapto Surjono*[1] & *I Gde Budi Indrawan*[1]

[1] Gadjah Mada University, Department of Geological Engineering, Yogyakarta, Indonesia.
E-mail: leandropceron@gmail.com; sugengssurjono@ugm.ac.id; igbindrawan@ugm.ac.id.

Abstract: In shale oil/gas exploration, using the Brittleness Index to identify sweet spots has become standard. This practice may incur inaccuracies when done inappropriately. This work used basic statistics and scatterplot analyses to identify trends and performance of four brittleness indexes. In the results, the indexes seemed similar in the well-logs with higher values in sandstone lithologies. The sensitivity to the parameters such as Total Organic Carbon, Porosity and Mineralogy, and fluid content varied among the indexes. The relation of the brittleness to the rock properties is mostly linked to the design features of the indexes. Brittleness Index selection should be done considering that some properties can affect the values positively or negatively. This work explains the brittleness index application more practically regarding the basic considerations to be included in shale plays evaluation.

Keywords: Shale gas; well logs; total organic carbon; reservoir geomechanics; mineralogy; multiple linear regression.

Resumo: Na exploração de petróleo/gás de lutito o uso do Índice de Fragilidade para identificar pontos-ideais tornou-se padrão. Esta prática pode ser imprecisa feita inapropriadamente. Este trabalho usou estatísticas básicas e gráficos de dispersão para identificar tendências e desempenho de quatro índices de fragilidade. Nos resultados, os índices pareceram similares nos registros e com valores mais altos em litologias de arenitos. A sensibilidade para parâmetros como o Carbono Orgânico Total, Porosidade, Mineralogia e fluido, variou entre os índices. A relação da fragilidade com as propriedades da rocha está principalmente ligada às características de desenho dos índices. A seleção do índice de fragilidade deveria ser feita considerando que algumas propriedades podem afetar de maneira positiva ou negativa. Desde este trabalho, a aplicação do índice de fragilidade é entendida em uma forma mais prática com respeito às considerações básicas a incluir na avaliação de Plays de lutitos.

Palavras-chave: Gás de folhelhos; registros de poço; carbono orgânico total; geomecânica de poços; mineralogia; regressão linear múltipla.

Recebido: data: 12/2023
Aceito: data: 05/2024
Publicado: data: 05/2024

1. Introduction

In the last decade, different factors have contributed to energy instability and uncertainty. Lately, the denominated shale 3.0 has been called out to be an alternative to salvage the panorama (Wright, 2012; Feder, 2020; Peña, 2022a). In unconventional exploitation, undoubtedly more challenging and complex than the conventional reservoirs (Zoback & Kohli, 2019), different methodologies are used to screen these plays (Zou, 2017). Since the early stages of shale oil/gas, a widely used method has been the evaluation of the Brittleness Index (Zhang *et al.*, 2016), which is assumed to be linked to the rock properties favourable for stimulation, i.e., hydraulic fracturing, and in some cases is taken as one of the six main parameters for defining the “sweet-spots” (Zou, 2017).

Using the Brittleness Index as an indicator of sweet spots requires assumptions to be adopted. Therefore, this implies inspecting to what extent the Index reflects the likelihood of intervals promising for stimulation (Rickman *et al.*, 2008; Chen *et al*., 2014; Jin *et al.*, 2015; Pan *et al.*, 2020). In this sense, an investigation into the controlling factors of the Brittleness Indexes should be carried out, specifically, its relationship with the mineral and fluid content, porosity, and the sync with the Total Organic Carbon. Previous works done on the subject have handled this analysis; nevertheless, with no detail in the relation of Brittleness to all those parameters mentioned beforehand (Chen *et al.*, 2014; Pan *et al.*, 2020). This work is intended to evaluate five Brittleness Indexes (Altindag, 2003; Rickman *et al.*, 2008; Chen *et al.*, 2014; Jin *et al.*, 2015; Pan *et al.*, 2020), with well-log data on a mudstone source rock interval (ConocoPhillips, 2011a; 2011b), and to present relative comparations amongst the indexes using statistics and scatterplots analysis (Bonamente, 2017).

2. Study Area

2.1 Geological Context

The location of the study area is in the Browse Basin, offshore of the Northwest Shelf, Australia, in the Caswell Sub-Basin (ConocoPhillips, 2011b) are shown in Figure 1.

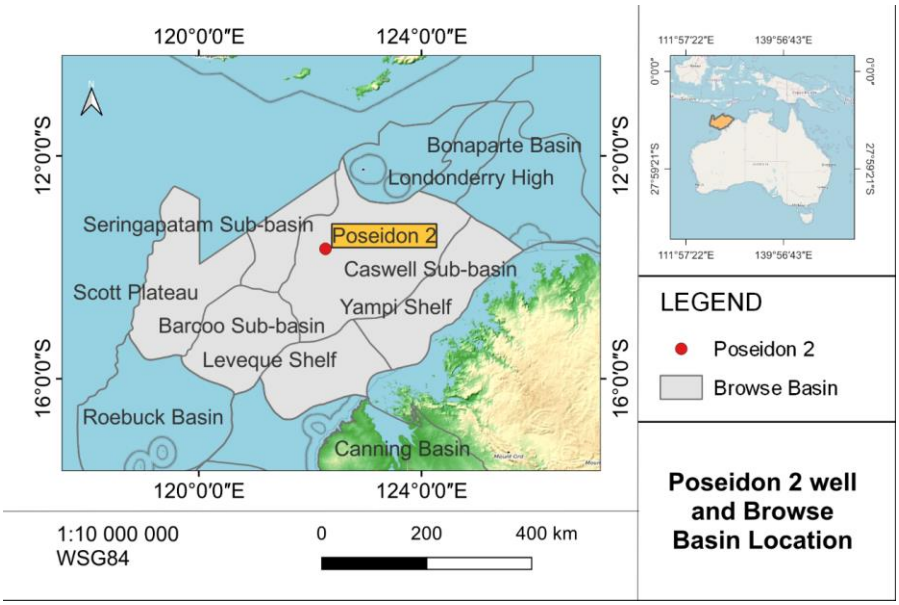

Figure 1. Location of the Poseidon 2 well within the Browse Basin with basemaps from OpenStreetMaps (https://www.openstreetmap.org/copyright). Well data from ConocoPhillips (2011b). Basin Features adapted from Raymond *et al.* (2018).

Figura 1. Localização do poço Poseidon 2 dentro da Bacia Browse com mapas base de 'OpenStreetMaps (https://www.openstreetmap.org/copyright). Dados de poço de ConocoPhillips (2011b). Características da bacia adaptadas de Raymond et al. (2018).

The structures limiting the basin are: It is side-to-side to the Yampi and Leveque Shelves; has continuous frontiers to the Southwest, Roebuck Basin with the Rowley Sub-basin and also to the Northeast, Bonaparte Basin with the Vulcan Sub-basin. To the Southeast, The Kimberly Block to the Norwest, the Scott Plateau, and the Argo Abyssal Plain (ConocoPhillips, 2012). The well has a total depth of 5356.0mMDRT (5334.2mTVDSS) with reservoir objectives Plover and Montara formations (sandstones). (ConocoPhillips, 2011b).

The interval of study it is within the plover formation is divided into two distinct geological units, the Plover Top Volcanics and the Plover Top Reservoir (ConocoPhillips, 2011b). The Plover Formation, Lower – Middle Jurassic age sediments, is mainly composed of sandstone, mudstone, and coal and these materials were accumulated in a deltaic and coastal plain environmental setting (Geoscience Australia, 2021a). This interval of study, in the Poseidon 2 well, which is at depths of 5119.43 m to 5220.6 m, was classified into 10 OBMI lithofacies, divided mainly into mudstones and sandstone lenses, and the facies associations into two, FA1 – A and FA1 – B ConocoPhillips, 2011b. The FA1 facies association is for thick argillaceous successions interpreted as marine mudstones from a shelf environment and the suffixes A and B refers to carbonate content differentiation, the B having a higher load than A (ConocoPhillips, 2011b).

The source rocks in the Plover Formation are mainly gas-prone with a maturity in the Caswell Sub-Basin that goes over 2 Vitrinite Reflectance (%Ro), presenting a median Total Organic Carbon (TOC) of 1.8% (Palu *et al.,* 2017).

3. Materials and Methods

The data for this work was obtained from two sources, the raw data from the National Offshore Petroleum Information Management System (NOPIMS) from Geoscience Australia, which is © Commonwealth of Australia and is provided under a Creative Commons Attribution 4.0 International License (Geoscience Australia, 2021b); and the pre-processed data by e-mail to the authors by Occam Technology Pty. Ltd. (2022). For the statistical analysis, the software R v.4.2.0 (R Foundation for Statistical Computing, 2022); and for the well-log data processing the software Interactive Petrophysics (IP) (Geoactive Limited, 2022).

In Figure 2, the general workflow applied in this research is shown. The first major step was to estimate the petrophysical parameters to evaluate the interval and the TOC, which was used as a reference to indicate organic richness. The second major step was to obtain Young's and Poisson's elastic modules, and in the last part, the calculations of the different brittleness indexes were done. In the brittleness evaluation section of the workflow, the indexes marked by a red shadow were normalized and cross-plotted against TOC, Porosity and Mineral Content, and fluid saturation. Also, a possible relation between OBMI Lithologies and the previous analyses. In addition to this, there were created and discretised ranges of TOC and fluid saturation into four sections and the arithmetic means (Bonamente, 2017) of the brittleness in those ranges were evaluated in order to understand deeply the characteristics presented.

Conventions in Figure 2 are as follows: Blue ellipses, start and end; blue circle with vertical and diagonal cross, joint and division of action flow; grey circle, in-page connector; grey parallelogram, input data; blue and red rectangles, process.

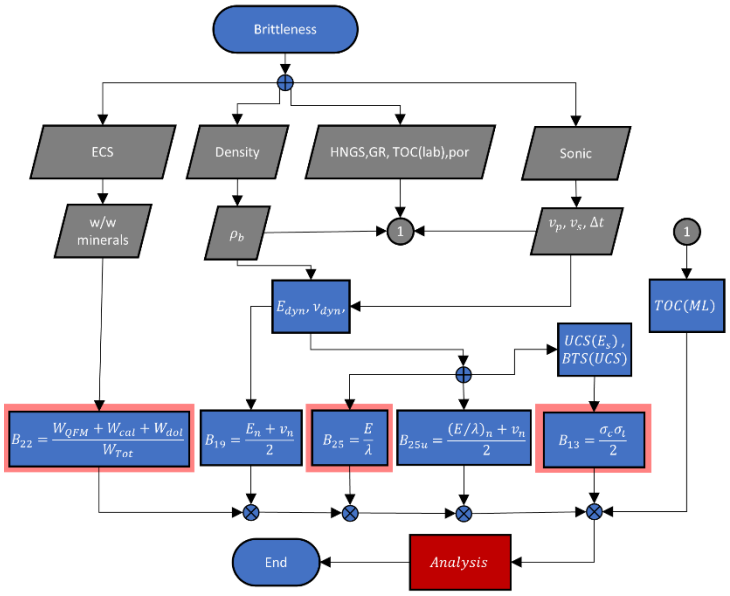

Figure 2. Methodology flowchart.

Figura 2. Fluxograma da metodologia.

3.1. Total Organic Carbon Estimation

To estimate the TOC in the well under study, the closest available laboratory TOC data was used as an input to create a multilinear regression model (Huang *et al.*, 2015). This data came from the Poseidon 1 well, which was determined by Rock-Eval Pyrolysis, and is located approximately 6 km in the Northeast direction (ConocoPhillips, 2010). Correlation between wells is implemented using the zonation identified by ConocoPhillips (2011a, 2011b), where similar facies are identified along well intervals. Considering their shared sedimentary paleoenvironment setting (Rollet *et al.,* 2018), log curve combinations sharing the same patterns are interpreted as homologous lithofacies between the reference well and the studied well.

Table 1 shows the parameters used for Multiple Linear Regression Analysis (MLRA) with data from Poseidon 1 (ConocoPhillips, 2010). The Total Organic Concentration is given in weight percentage, i.e., the mass of organic carbon fraction over the total mass of the rock in the interval evaluated. The parameters were: Measured Depth from Rotary Table (MD), 26.40 MAMSL – meters above mean sea level, TOC, Uranium Content (U), Bulk Density (BD), Compressional Wave Slowness (DTC), Gamma Ray (GR).

Table 2. Data for multilinear regression from Poseidon 1 well. Adapted from ConocoPhillips (2010).

Tabela 1. Dados para a regressão linear múltipla do poço Poseidon 1. Adaptada de ConocoPhillips (2010).

MD (m)	TOC (wt%)	U (mol/m3)	BD (kg/m3)	DTC (us/m)	GR (gAPI)
4684	2.11	0.01607	2576.98	303.35	172.75
4702	2.1	0.01555	2691.86	215.81	92.62
4726	1.44	0.0007933	2647.68	226.74	12.60
4831	1.25	0.009849	2701.70	200.55	82.40
4924	1.62	0.007024	2729.30	233.90	111.34

The total Organic Carbon estimation for the well under this study, Poseidon 2, was done using a MLRA with a previous screening using a Pearson correlation discrimination step (R Foundation for Statistical Computing, 2022). The linear resulting models were subjected to ANOVA testing and the final model was tested in a t-welch two tails model with a 95% confidence interval (R Foundation for Statistical Computing, 2022). Figure 3 shows the well composite of Poseidon 1 with the laboratory data of TOC.

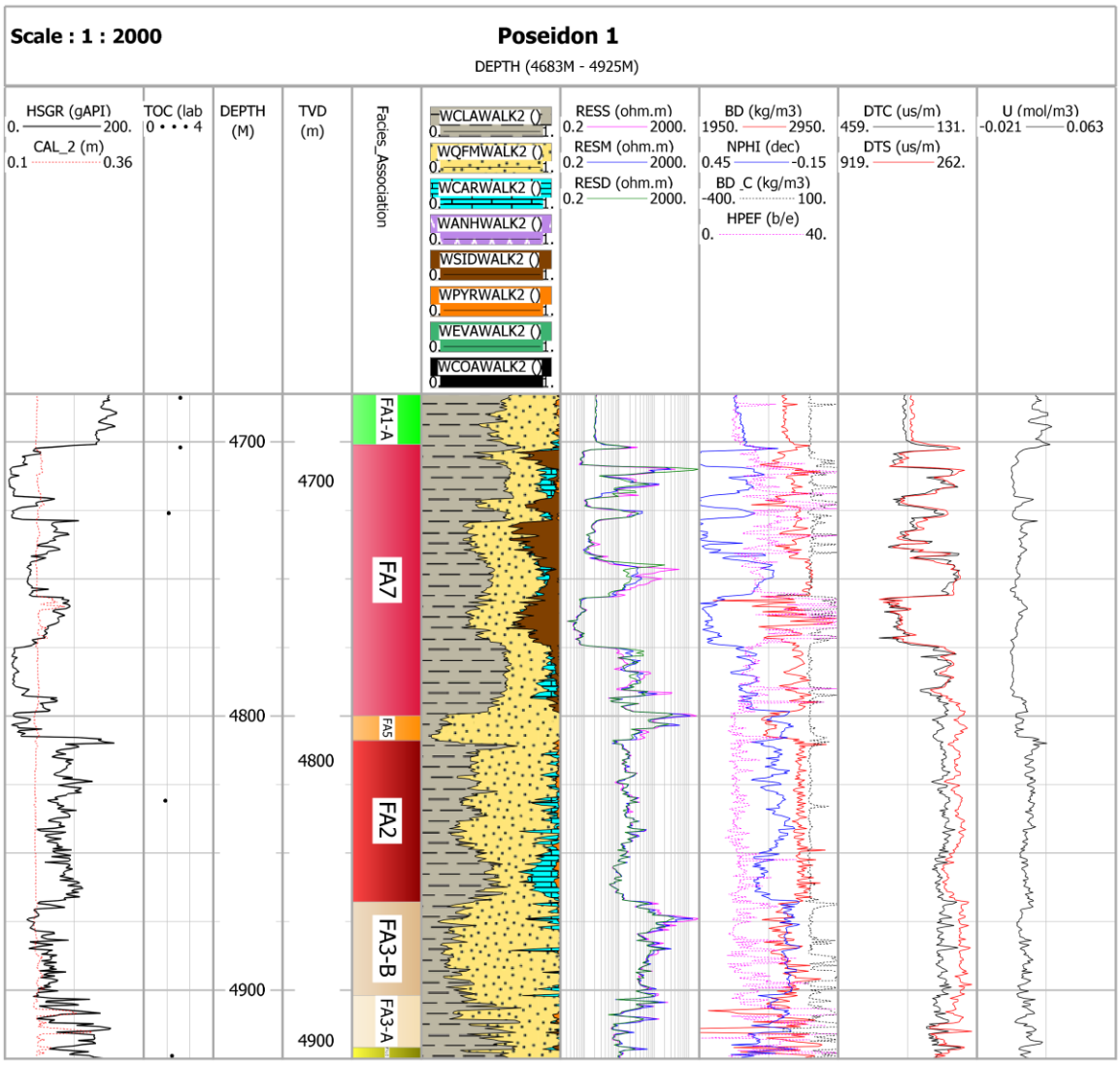

Figure 3. Well-log composite in the Poseidon 1 well with TOC data.

Figura 3. Registro do perfil composto do poço Poseidon 1 com dados de COT.

3.2. Elastic Moduli, Unconfined Compressional and Tensile Strength

The Elastic moduli were estimated using formulations for the dynamic Young's Modulus and the Poisson's Ratio (Fjær *et al.*, 2008). The static Young's Modulus correlation implemented was the one from (Chang *et al.*, 2006). For the estimation of the Unconfined Compressional Strength correlations to Young's Modulus were used (Chang *et al.*, 2006; Peña, 2022b), as they were established to have a good fit for the relatively high volumes of quartz in and for the low quartz content, e.g., high clay/shale per correspondent lithology intervals (Peña *et al.*, 2023). The Tensile Strength was estimated using the formulation found by (Ribeiro *et al.*, 2016).

3.3. Brittleness Estimations

The brittleness indexes evaluated in this work were the ones shown in: B13 in equation (1) (Altindag, 2003), with Unconfined Compressional Strength (UCS) and Tensile Strength (BTS).

$$B_{13} = \frac{UCS*BTS}{2} \quad (1)$$

B19 in equation (2) (Rickman *et al.*, 2008; Jin *et al.*, 2015), with Normalised Young's Modulus (En) and Normalised Poisson's Ratio (vn);

$$B_{19} = \frac{E_n+\upsilon_n}{2} \quad (2)$$

B22 in equation (3) (Jin *et al.*, 2015), with the Weight Fractions of Quartz, Feldspar, and Micas (QFM), Calcite (Cal), and Dolomite (Dol).

$$B_{22} = \frac{W_{QFM}+W_{cal}+W_{dol}}{W_{Tot}} \quad (3)$$

B25 in equation (4), with Dynamic Young's Modulus (E) and the First Lamé Parameter (λ) (Chen *et al.*, 2014);

$$B_{25} = \frac{E}{\lambda} \quad (4)$$

B25u in equation (5) (Pan *et al.*, 2020), with the Normalised Young's Modulus – First Lamé Parameter (E⁄λ)_n and the Normalised Poisson's ratio.

$$B_{25u} = \frac{(E/\lambda)_n+\upsilon_n}{2} \quad (5)$$

The brittleness denominated here as B13, B22, and B25 were normalised in order to be compared to the other indexes, which can be considered already normalised, i.e., B19 and B25u. The new denominations for normalised brittleness have the suffix "n", e.g., B22n. The units resulting from this processing, and for all the indexes were dimensionless [DN].

4. Results and Discussion

4.1. Total Organic Carbon (TOC) from Multiple Regression Analysis

The TOC Multiple Regression Analysis resulted in a model as in the equation (6) for the Poseidon 1 well. The results of the Pearson Correlation implemented are shown in Table 2. The selection of the linear model was done considering that the variables physically linked to other properties rather than TOC were excluded. To fit the TOC to an appropriate model it takes into account the recommendations according to Huang *et al.* (*2015*), where high values of Ro make the model based upon $\Delta \log R$ imprecise, as the Caswell Sub-Basin has values of %Ro over 2.

Table 2. Pearson Correlation for the TOC evaluation in the Poseidon 1 well.

Tabela 2. Correlação de Pearson para a avaliação do COT no poço Poseidon 1.

	TOC	U	BD	DTC	GR
TOC	1	0.75	-0.46	0.62	0.63
U	0.75	1	-0.28	0.39	0.8
BD	-0.46	-0.28	1	-0.82	-0.36
DTC	0.62	0.39	-0.82	1	0.71
GR	0.63	0.8	-0.36	0.71	1

Multi-collinearity between Uranium logging (U) and Gamma Ray curve (GR) from Table 2 excluded these two variables into the model. The chosen variables were the sonic (DTC) and Bulk Density (BD), and after a control step by the ANOVA one was eliminated from the model. The chosen variable was the Bulk Density, because as a TOC indicator the Bulk Density is correlated and this curve is also good indicator, which decreases with the increase of TOC (Huang *et al.*, 2015). The equation (6) was applied for the estimation of the TOC in the interval of the Poseidon 2 well.

$$TOC(BD) = -3.01BD + 9.74,\ R^2 = 0.2121 \quad (6)$$

4.2. Well-log composite

In Figure 4, all the Brittleness curves, the TOC, Porosity and OBMI Lithologies with the Facies Association in the Poseidon 2 well are shown. In general, all the brittleness curves follow a similar trend, higher in the upper section of FA1 – A and lower at the bottom. The Brittleness values for FA1 – B are lower relative to the first facies associations. In this second lower interval, the B22n decreases with deep whilst the other keeps steady values. All the brittleness seems to experience changes in porosity and gas saturation, having greater value with their increments; nevertheless, the brittleness in regard to the TOC, apparently, does not experience big changes.

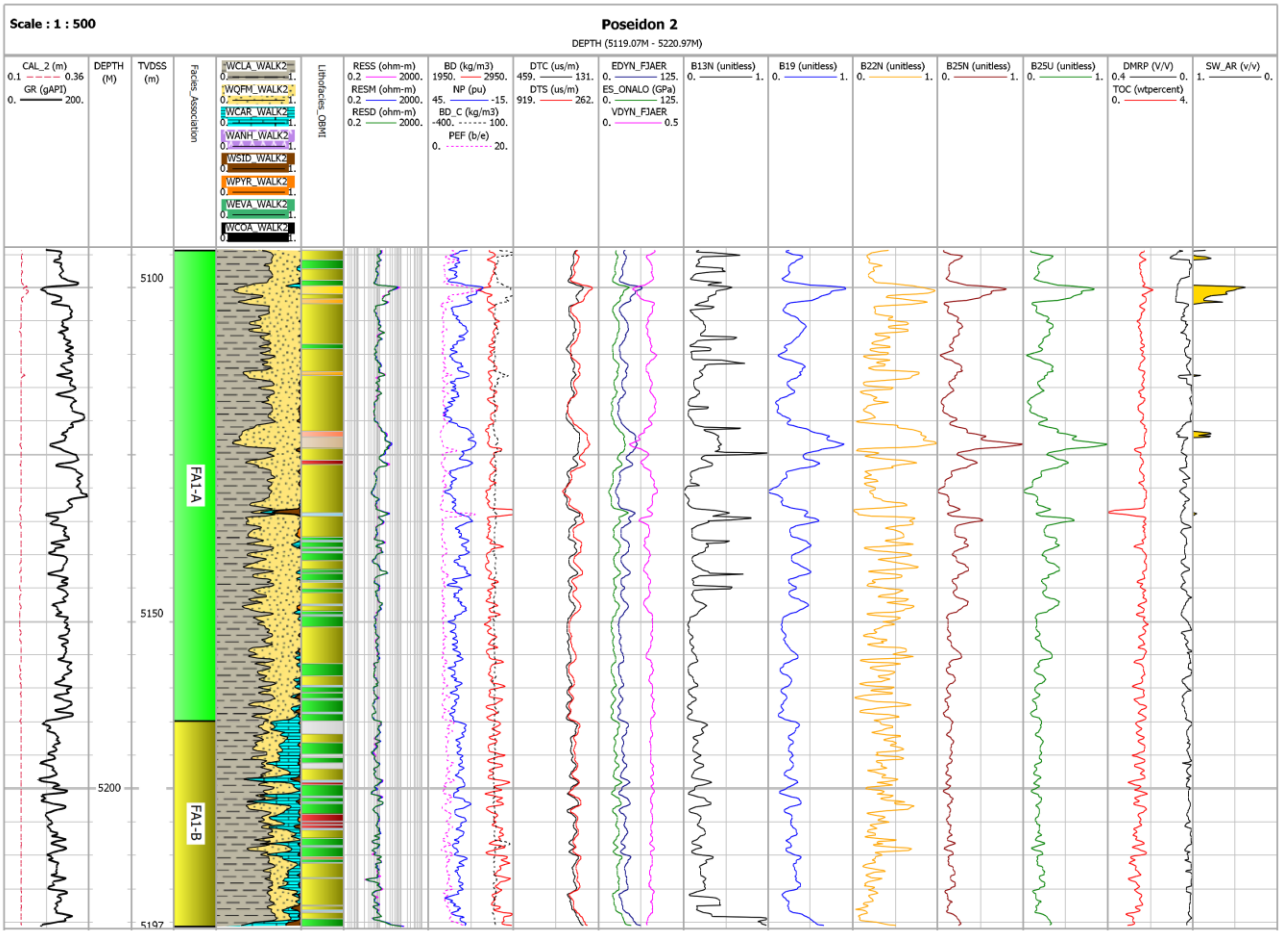

Figure 4. Well-log composite in the Poseidon 2 well.

Figura 4. Registro do perfil composto do poço Poseidon 2.

4.3. Brittleness and TOC

In the Table 3 is summarised the results of the calculations done on the Brittleness Indexes evaluated in this work with respect to the estimations of the ranges of TOC, in the Poseidon 2 well. The 4 ranges chosen were numbered from 1 to 4, starting at 0 and ending in 2.5 of TOC, totalling 600 logging curve sample points from the mudstone lithofacies; the TOC is indicated in weight percentage, wt%, and the Brittleness in dimensionless units, DN.

Table 3. Brittleness arithmetic means and TOC ranges.

Tabela 3. Médias aritméticas do Índice de Fragilidade e intervalo de COT.

		Range			
		1	**2**	**3**	**4**
TOC range [wt%]	Lower Bound	0	0.54	1.08	1.61
	Upper Bound	0.54	1.08	1.61	2.15
Mean [DN]	B13n	0.47	0.37	0.34	0.19
	B19	0.46	0.40	0.36	0.28
	B22n	0.03	0.22	0.28	0.35
	B25n	0.18	0.19	0.16	0.18
	B25u	0.23	0.23	0.20	0.23

From Table 3, major trends identified based upon the arithmetic means of the ranges in B19 and B13n indicates that are inversely correlated to the TOC, which is sharply observable in B13n. These results are in concordance with the basic design definitions of the B13n (Zhang *et al.*, 2016; Altindag, 2003) and B19 (Zhang *et al.*, 2016; Rickman *et al.*, 2008; Jin *et al.*, 2015) that were focused on the mechanical properties of the brittleness rather than the organic matter content; moreover, the reduction is because TOC in terms of mechanical behaviour is similar to clays in unconventional reservoirs (Zoback & Kohli, 2019). The rest of the indexes, B22n, B25n, and B25u are proportional to TOC, and in the case of B22n, it shows a stepped increase as the TOC augments in richness. In B25n and B25u there are slight increments that becomes more apparent after 1.6 wt% in TOC. In the case of B22n, the strong climbing can be explained by the quality of the source rock, in the upper FA1 – A section where the QFM content fraction is bigger along with porosity in shallower sections, indicating a correlation between the Quartz, Feldspar, and Mica fraction and TOC. This correlation has been identified in shale gas, but is not always present (Ibad & Padmanabhan, 2022).

The Figure 5 shows the brittleness versus the TOC concentration in weight percentage. These scatterplots were depicted to analyse visually the brittleness of the mudstone intervals, which totaled 600 logging curve sample points. In Figure 5a, B13n index presents a similar behaviour to B19 with respect to TOC; moreover, it is clear for any percentage of Total Organic Carbon the inverse relation of B13n and TOC, with a negative sharp trendline. B19 (Fig. 5b) has a less pronounced negative trendline.

In the case of B22n (Fig. 5c), the relation to TOC is directly proportional and it is positive contrary to the B13n and B19, confirmed by a very steep trendline. B22n presents preference to be correlated directly to the laminated muds lithofacies, olive green in colour, rather than the other facies as for example muds poorly stratified (green colour). Also, with

the gain in clay minerals, and reduction of QFM within the intervals of calcareous mudstones (Fig. 4, zone FA1-B) B22N shrinks, indicated by a mild slope compared to the other lithofacies trendline slopes in this index.

In Figure 5d and Figure 5e, B25N and B25U, both are directly linked to TOC; however, with far weaker slope trendlines than the one presented in B22N. A notable difference is the preference of these two indices to preferentially be directly correlated to calcareous mudstones (opposed to what B22N indicates), independently of clay mineral content. B25N and B25U does not present remarkable differences rather than slightly more positive correlation to TOC in the latter.

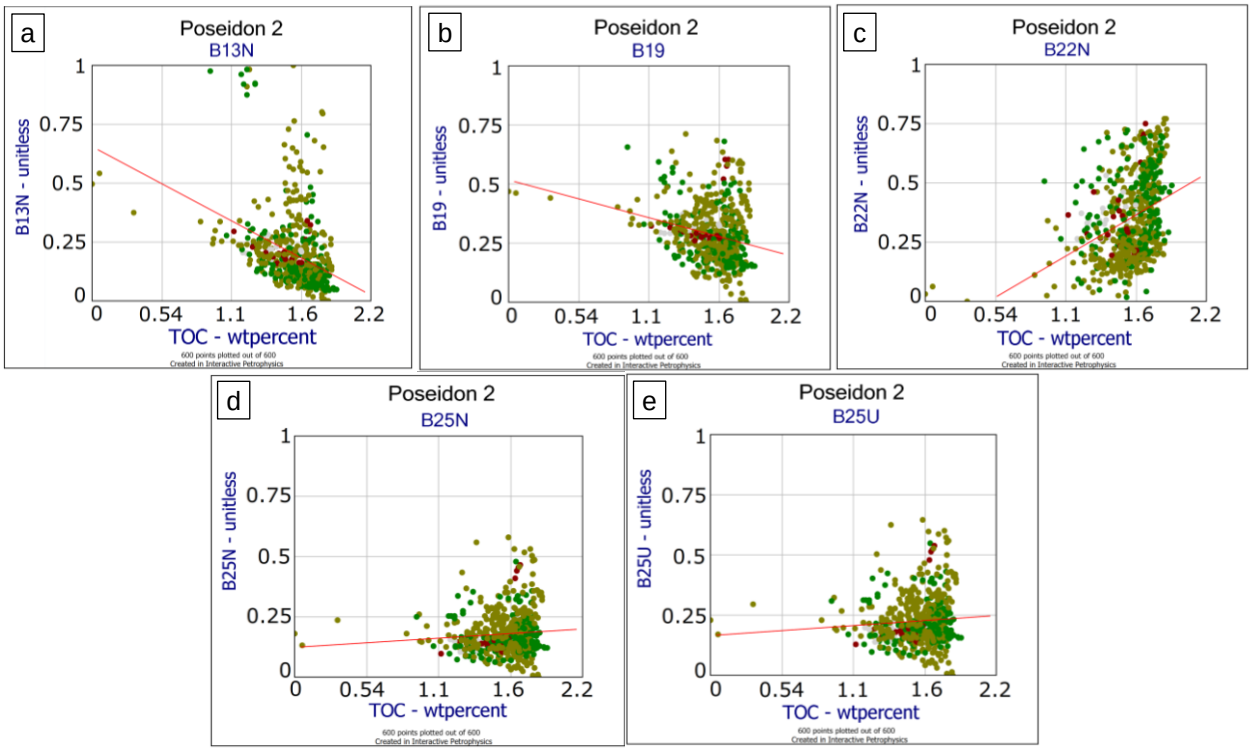

Figure 5. Brittleness vs TOC in mudstones from 600 logging curve sample points. (a) B13N (b) B19 (c) B22N (d) B25N and (e) B25U.

Figura 5. Índice de Fragilidade vs COT em lamitos de 600 pontos de amostragem de curvas de perfilagem. (a) B13N (b) B19 (c) B22N (d) B25N e (e) B25U.

4.4. Brittleness, mineralogy, and porosity

Figure 6 shows the relation of the two brittleness indexes B19 (Fig. 6a) and B25u (Fig. 6b) with reference to the porosity, total porosity (DMRP), and the WQFM mineralogy, Weight fraction of Quartz, Feldspars, and Micas obtained from the Elemental Capture Spectroscopy (ECS) tool. The WQFM fraction is coloured from cold to a warm colour, with the highest values in the warm spectra. In B19, there is a correlation between the increase of the porosity and the WQFM, where their joint increase is paired with brittleness B19 rise, this trend is more easily seen over porosities of 2%. This relationship is consistent in the sandstone-related lithologies and less even in the mudstone group, where the laminated mudstone lithologies still maintain, seemingly, the relation of Porosity-WQFM-Brittleness behaviour. B25u, shows an identifiable confident relation of Brittleness to porosity and WQFM and this trend disperses a bit with higher porosities. The B25u in this interval shows a better fit in the mudstones to grow in porosity with WQFM than the other indexes; the Porosity-WQFM-Brittleness connection is held. The B25n has a similar trend to B25u, but a

lesser magnitude, as is seen in the TOC behaviour between B25n and B25u. Red arrows in Figure 6 indicates the overall increase in Brittleness along with WQFM and porosity, with more consistency in Figure 6b (B25U).

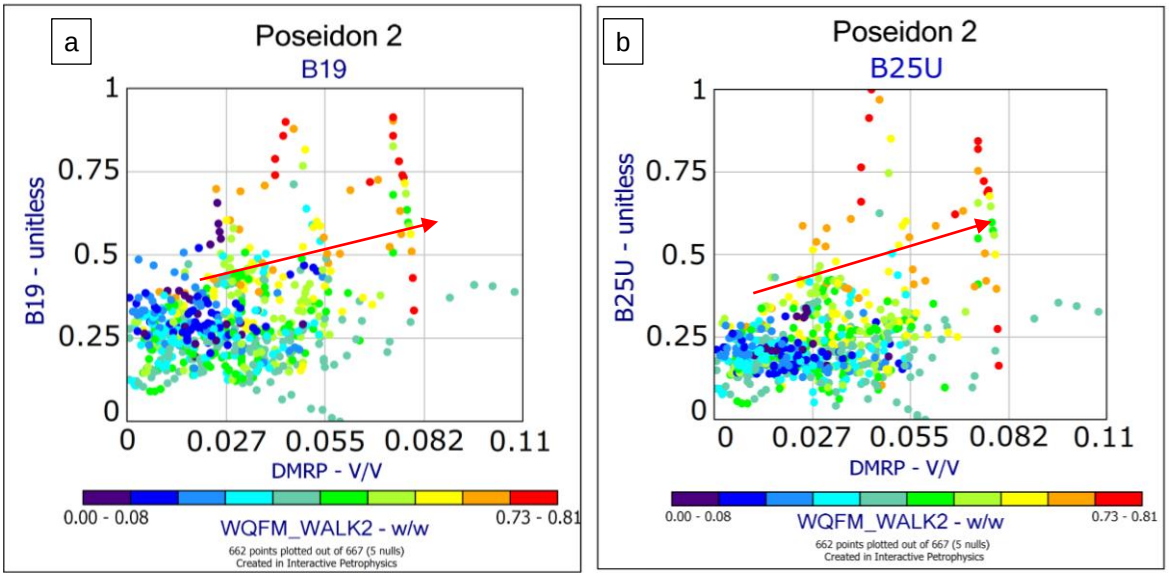

Figure 6. Brittleness vs Porosity with WQFM fraction in colour (a) B19 (b) B25u.

Figura 6. Índice de Fragilidade vs Porosidade com 'fração em peso de Quartzo-Feldspatos-Micas' WQFM em cores (a) B19 (b) B25u.

Overall, in the B13n, there is no correlation of brittleness to porosity and QFM. In the case of the B22n, there is no relation between the porosity and Brittleness; however, it can be seen that the rise of WQFM is paired to the Brittleness: larger WQFM results in larger B22n. By lithofacies groups, the sandstone lithologies showed a proportional relationship, but only for porosities major than 6% and with great WQFM content.

To investigate deeper into the influence of mineralogy on the Brittleness Indexes evaluated in this work, the Brittleness's were plotted against the WQFM, with colouring the WCLA (Weight Fraction of the Clay Minerals, warmer colour for higher values) and with the size of every point to the constitutive WCAR (Weight Fraction of Carbonate Minerals) (Figure5); considering the fact that these three minerals are the most abundant, as seen in Figure 4, track 5 ECS mineralogy. In Figure 5a and Figure 5b, blue polygon encircle the calcareous muds and red polygon encircles sandstone lithofacies; the rest of the dots corresponds to the other lithofacies, mostly laminated and poorly stratified muds, found in the interval studied.

In Figure 7a, the B19 has a distinguishable relationship with the WQFM presence and also with the WCAR, their increase signifies a gain in B19 values; on the contrary, the clay diminishes it. For the sandstone lithologies (red dashed polygon), the index is positively related to the WQFM and for the mudstones this relationship is not present, it is just linked in a minor way to the carbonate presence. The B25n, is highly correlated to the presence of Quartz, Feldspar, and Micas, with growing B25n as the WQFM rises. Its relationship is low in carbonate presence and in the clay materials the B25n is reduced.

In the mudstones B25 presents more consistency, even showing a oppose relation between clay and brittleness, more clay percentage represents more brittleness. As it was witnessed in the results beforehand with the TOC, B25u exhibits the same behaviour as the B25n, but with bigger differences in the magnitude range.

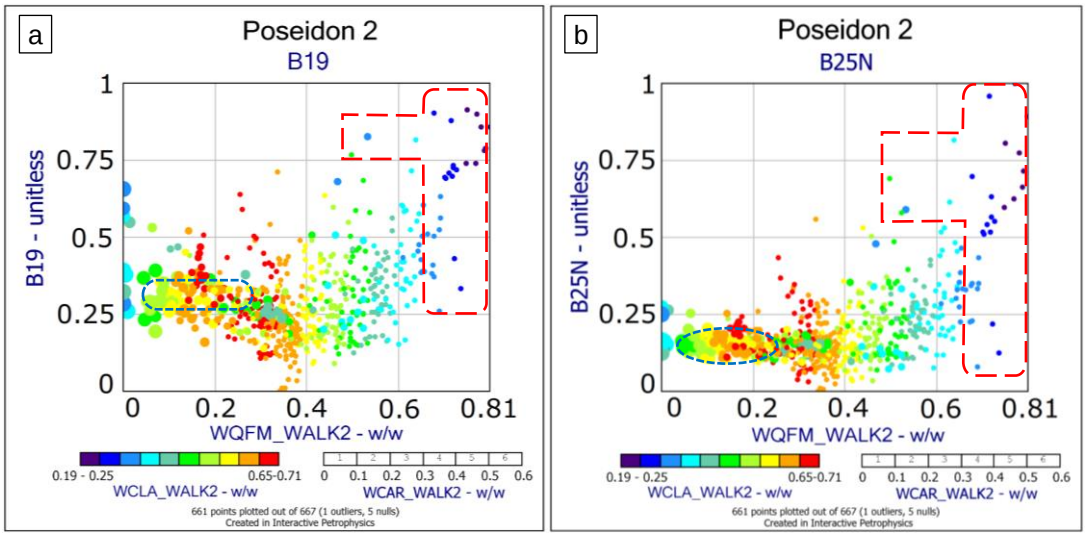

Figure 7. Brittleness vs WQFM, with WCLA in colour and with WCAR in size point (a) B19 (b) B25n.

Figura 7. Índice de Fragilidade vs WQFM, com WCLA em cores e com 'fração em peso de carbonatos' WCAR em tamanho de ponto (a) B19 (b) B25n.

4.5. Brittleness and Gas Saturation

In Table 4 is summarised the arithmetic means of the Brittleness in relation to the Gas Saturation per range, gas saturation estimated with the methodology use in Peña (2022b, Appendix B) and considering a porous system of gas-water; this in four ranges starting in 0% and ending at 62% in volume. In total 38 points were analysed, which existed in the interval. From this table, it is seemed that the best performance is held by the B22n and the lowest for the B13n, with intermediates B25n, B25u, and B19. This last one is the second-best regarding gas sensitivity.

Table 4. Brittleness arithmetic means and ranges of Gas Saturation.

Tabela 4. Médias aritméticas do índice de fragilidade e intervalos de saturação de gás.

		Range			
		1	**2**	**3**	**4**
Sg range [v/v]	Lower Bound	0.00	0.16	0.31	0.46
	Upper Bound	0.16	0.31	0.46	0.62
Mean [DN]	B13n	0.31	0.34	0.35	0.47
	B19	0.42	0.60	0.64	0.84
	B22n	0.45	0.65	0.80	0.89
	B25n	0.24	0.43	0.52	0.71
	B25u	0.29	0.50	0.57	0.76

In Figure 8 is shown the different Brittleness respect to the decreasing water saturation (increasing gas saturation). The water mentioned here is no Water Bound into the porous space (in this study, the threshold is 100% in water saturation, Sw). The interval has been identified as gas/water saturated (ConocoPhillips. 2011b).

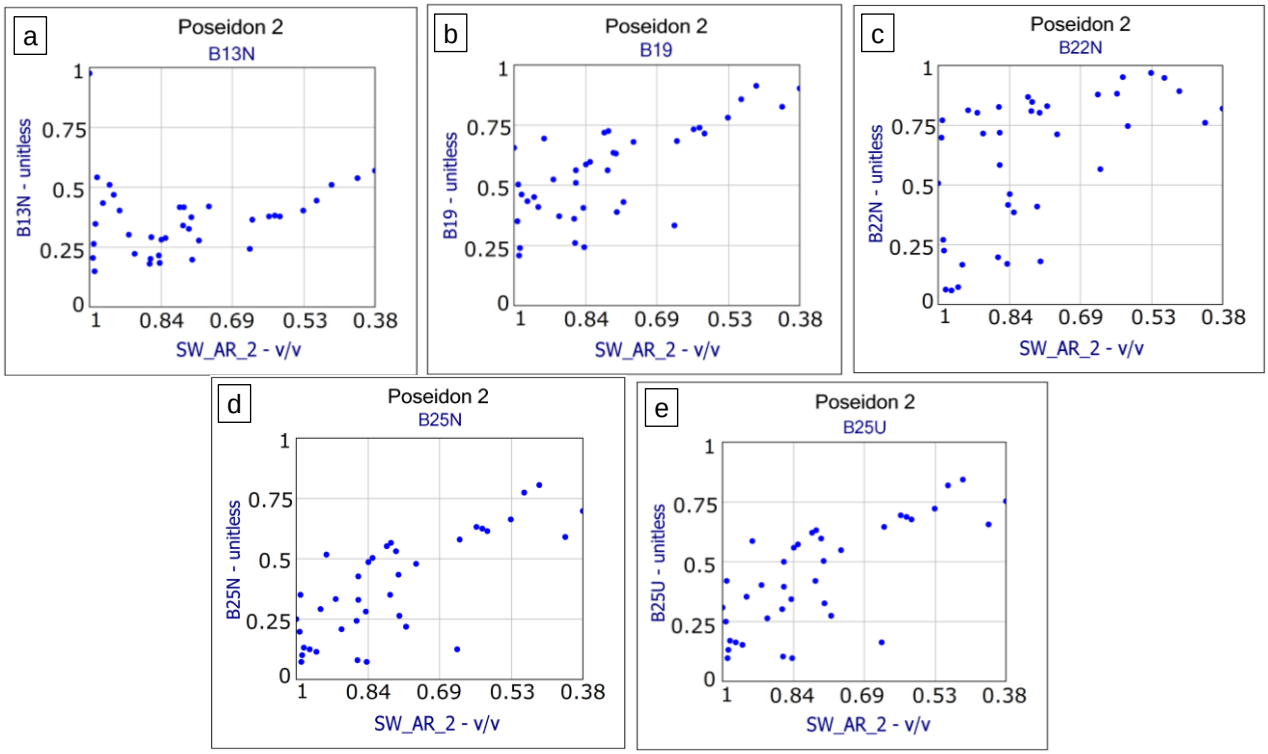

Figure 8. Brittleness vs Water Saturation (a) B13n (b) B19 (c) B22n (d) B25n (e) B25u.

Figura 8. Índice de fragilidade vs Saturação de água (a) B13n (b) B19 (c) B22n (d) b25n (e) B25u.

The B13n, in Figure 8a, is high with high water saturation, a trend that follows a parabolic-like relationship with the vertex over 0.5 in Sw (v/v) and to the peak at 40% of liquid saturation reaches a B13n of 0.6. This positive parabolic shape is held in both sandstone and mudstone lithofacies groups. In Figure 8b, B19 exhibits a clear inverse relation to Sw. The B19 starts with an average of 0.42 in 99% of Sw and ends with an average of 0.84 B19 at 40% Sw (60% Sg) and this linear like tendency is present in mudstone and sandstone groups in the facies association of the interval FA1. The maximum standard deviation all over the 4 interval ranges of Sw is 0.17. In Figure 8c, the B22n shows a proportional relationship like B19, but the points are more dispersed, especially in the high-water saturation zones. By lithofacies groups, in the mudstone group the trend is highly dispersed for high Sw and this lithofacies group presents values that range from 0.05 to 0.8 in brittleness in high Sw. The total standard deviation of Brittleness reaches 0.3.

The B25n in Figure 8d, like B19, shows a positive a clear relationship to the increase of the gas saturation. The difference is the magnitude of the values: for high water saturation, the B25n is almost 0.15 lower in normalized brittleness value and at the limit of the water saturation, approximately 0.62 in volume, the brittleness is 0.2 approximately. In Figure 8e, the B25u still follows the same path described in the previous B25n index, only augmenting the total value of Brittleness between 5% to 13% throughout saturation. The trend is maintained for the two lithofacies groups, and also the B25n and B25u show less dispersion in the high-water saturation (more than 70%) with values between 0.12 – 0.16 than B22n; the total standard deviation for B25n and B25u is almost equal for the two of them to 0.21.

Taking into account all the indexes, there is no ideal model that regards all the variables here mentioned, as stated by Zhang *et al.* (2016). The B19 utilizes the Young's Modulus and Poisson's Ratio in an arbitrary manner, normalizing them and taking 50/50 in percentage per elastic modulus (Rickman *et al.*, 2008; Jin *et al.,* 2015; Zhang *et al.*, 2016).

As it was seen in the section of the Total Organic Carbon, this index has no positive correlation, implying that using solely an analysis with B19 for identifying a pay-zone in an unconventional reservoir may ignore the organic matter presence and richness. A similar phenomenon is seen in B22n, as was previously discussed, the relationship to the organic richness must be demonstrated beforehand or simultaneously to have a better understanding of the section evaluated [30]. In Zhang *et al.* (2016), the limitations of the B22 index is also mentioned, as it was witnessed previously in the section about porosity and mineralogy, the index does not necessarily reflect consistency. This may be caused by different lithologies and sections that can have the same mineralogy and different porosity, also compaction and diagenesis effects that are not detected by the index (Zhang *et al.*, 2016): in this study, this was observed by the widely scattered interaction with porosity and the high correlation to the TOC.

The index normalization of the B25 (B25n) produces trends similar to the B25u (Fig. 7d and Fig. 7e), the latter was specifically proposed to overcome the lack of sensitivity of the B19 index to high porosity and the Total Organic Carbon (Pan *et al.,* 2020), but here is considered an improvement of the B25 for its fit. Despite this, in the low porosities presented in the interval evaluated, the B19 demonstrated similar performance (with the exception of the negative relationship to the TOC) to the B25u. In a wide interval, i.e., covering more than one lithology type in several formations, the selection of the minimum and maximum values of the index for normalization can have a drastic impact on the results of the indexes, as it was seen in Peña (2022b), where the indication of the B25n brittleness in potential pay-zones was negligible whereas other indexes indicated target zones.

In Peña (2022b), it was established that to get a better evaluation of intervals for stimulation, more criteria additional to Brittleness should be added to improve the results. These may be the in-situ stresses, other rock mechanics variables such as Unconfined Compressed Strength and Tensile Strength, as well as Fracture Toughness, and the pre-identification of pay-zones under different cut-offs (Jin *et al.,* 2015; Peña, 2022b).

5. Conclusions

The conclusions reached using the workflow described in the methodology section of this work are the following:

The selection of a Brittleness Index in order to evaluate an unconventional play has to be done with care, considering the following: data available, the quality of the data, and the supporting methods in order to identify sweep-spots. There is some brittleness like B25n and B25u designed to perform better in specific conditions rather than other more general, like the B19.

The B13n index, as defined in this work, is the Index with the least performance and is not recommended when evaluating an unconventional play considering TOC, porosity, fluid saturation, and mineralogy.

The B22n is a good indicator of brittleness in terms of mineralogy and TOC, but it cannot be linked necessarily to the sweet-spots in unconventional resources as there has to be a positive relation of the WQFM and WCAR fraction to the TOC percentage, a condition that is not always present. Besides, the relation with respect to the Porosity is not consistent, and in regard to the gas saturation, there is a positive relation, but it is inconveniently scattered.

The B19 is overall the best indicator of Brittleness for sweet-spots; however, it fails to account for the presence of TOC in a positive correlation. The porosity and the mineralogy showed modest but consistent relationships with a positive trend between Brittleness and

these two parameters. This is the index with the second-best performance in gas sensitivity and taking into account the apparent lack of precision of B22n, the B19 index may be the best option related to gas sensitivity in low porosity intervals.

The B25n index is a specialized index designed to account for the porosity, TOC, mineralogy, and gas saturation and it shows a modest performance about all these properties. The normalization of the B25n changes the ranges of the index, making it similar to the one considered here, the updated version B25u, which was done to improve mainly the sensitivity to high porosities. In relatively low TOC and porosities, the normalized B25n and the B25u have equal trends, but in different magnitudes, also in low porosities, the weighted performance of the B25u is better than the B19, because this includes the TOC as a beneficial property for brittleness.

6. Recommendations

A similar analysis should be done on a well-characterized shale gas interval that may possess high variation of TOC and porosities as well as fluid saturation, in order to evidence in more detail, the benefits and pitfalls of the indexes presented here.

When implementing a shale play evaluation, i.e., brittleness index, it is highly recommendable to use more than one index. This is practically important, even though the one to be used is designed for such evaluation, the inclusion of other brittleness can give an estimation of reference. Also, the Brittleness should not be the only property when identifying sweet-spots, as the variables included may not be totally descriptive of the interval: properties such as in-situ stress magnitudes and directions, fracture toughness, tensile and compressive strength may help in this assessment.

Author contributions: Conceptualisation, K.L.P.C. and S.S.S.; methodology, K.L.P.C., and I.G.B.I; software, K.L.P.C., and S.S.S.; validation, K.L.P.C.; formal analysis, K.L.P.C; research, K.L.P.C; resources, K.L.P.C; data preparation, K.L.P.C; article writing, K.L.P.C; review, K.L.P.C, and I.G.B.I.; supervision, K.L.P.C., S.S.S., and I.G.B.I; financing acquisition, K.L.P.C. and S.S.S. All authors have read and agreed to the published version of the manuscript.

Conflict of interest: The authors declare that there is no conflict of interest.

References

Altindag, R. 2003. Correlation of specific energy with rock brittleness concepts on rock Cutting. *Journal of the Southern African Institute of Mining and Metallurgy,* 103(3): 163-172. https://hdl.handle.net/10520/AJA0038223X_2948

Bonamente, M. 2017. *Statistics and Analysis of Scientific Data*. 2nd ed. New York, Springer, 318p.

Chang, C., Zoback, M.D. & Khaksar, A. 2006. Empirical relations between rock strength and physical properties in sedimentary rocks. *J. Pet. Sci. Eng.*,51(3): 223-237. https://doi.org/10.1016/j.petrol.2006.01.003

Chen, J.; Zhang, G.; Chen, H. & Yin, X. 2014. The construction of shale rock physics effective model and prediction of rock brittleness. *In:* Annual SEG Meeting, 84, Oct. 2014, Denver, Colorado, USA. *SEG Tech. Program Expand. Abstr. 2014,* Denver, p. 2861-2865. https://doi.org/10.1190/segam2014-0716.1

ConocoPhillips. 2010. *Poseidon 1. WCR (basic): Well Completion Report.* National Offshore Petroleum Information Management System (NOPIMS), ConocoPhillips, Volume 1: Basic Data, 1133p. (Released Report). Available in: < https://dnxxuwuw8tglo.cloudfront.net/Wells/P00685602.zip >. Accessed in: Dec. 2021.

ConocoPhillips. 2011a. *Poseidon 2. WCR (Basic): Well Completion Report*. National Offshore Petroleum Information Management System (NOPIMS), ConocoPhillips, Volume 1: Basic Data,1446p. (Released Report). Available in: < https://dnxxuwuw 8tglo.cloudfront.net/Wells/P00688589.zip >. Accessed in: Dec. 2021.

ConocoPhillips. 2011b. *Poseidon 2. WCR (interpreted): Well Completion Report.* National Offshore Petroleum Information Management System (NOPIMS), ConocoPhillips, Volume 2: Interpretative Data, 990p. (Released Report). Available in: < https://dnxxuwuw8tglo.cloudfront.net/Wells/P00707041.zip >. Accesed in: Dec. 2021.

ConocoPhillips. 2012. *WA-315-P & WA-398-P Browse Basin Western Australia: 2009 Poseidon 3D Marine Surface Seismic Survey Interpretation Report.* National Offshore Petroleum Information Management System (NOPIMS), ConocoPhillips, 43p. (Released Report). Available in: < https://dnxxuwuw8tglo.cloudfront.net/Surveys/P00696639.zip >. Accessed in: Dec. 2021.

Fjær, E.; Horsrud, P.; Risnes, R.; Holt, R. & Raaen, A. 2008. Petroleum Related Rock Mechanics. *In:* Developments in Petroleum Science, v. 53, 2nd ed. Elsevier Science, 491p.

Feder, J. 2020. *Unconventionals at a Crossroads: Where Do We Go from Here?* Available in: < https://jpt.spe.org/unconventionals-crossroads-where-do-we-go-here >. Accessed in: Aug. 2021.

Geoactive Limited. 2022. Aberdeen, United Kingdom, 2021 release. Available in: < https://www.geoactive.com/resources/ic-2021-latest-release >. Accessed in: Oct. 2022.

Geoscience Australia. 2021a. *Regional Geology of the Browse Basin*. Available in: < https://www.ga.gov.au/scientific-topics/energy/province-sedimentary-basin-geology/petroleum/acreagerelease/browse>. Accessed in: Nov. 2021.

Geoscience Australia. 2021b. *Copyright and Disclaimer Notice*. Available in: < https://www.ga.gov.au/copyright >. Accessed in: Nov. 2021.

Huang, R.; Wang, Y.; Cheng, S.; Liu, S. & Cheng, L. 2015. Selection of logging-based TOC calculation methods for shale reservoirs: A case study of the Jiaoshiba shale gas field in the Sichuan Basin. *Nat. Gas Ind. B*, 2(2-3): 155-161. https://doi.org/10.1016/j.ngib.2015.07.004

Ibad, S.M. & E. Padmanabhan, E. 2022. Inorganic geochemical, mineralogical and methane sorption capacities of Paleozoic shale formations from Western Peninsular Malaysia: Implication of shale gas potential. *Appl. Geochemistry*, 140:105269:1-20. https://doi.org/10.1016/j.apgeochem.2022.105269

Jin, X.; Shah; S.N.; Roegiers, J-C. & Zhang, B. 2015. An Integrated Petrophysics and Geomechanics Approach for Fracability Evaluation in Shale Reservoirs. *SPE J.*, 20(03): 518–526. https://doi.org/10.2118/168589-PA

Occam Technology Pty. Ltd. 2022. *Poseidon 2: Well Data.* Adelaide, Occam Technology Pty. Ltd. (Private Communication).

Pan, X.P.; Zhang, G.Z. & Chen, J. 2020. The construction of shale rock physics model and brittleness prediction for high-porosity shale gas-bearing reservoir. *Science*, 17: 658-670. doi: https://doi.org/10.1007/s12182-020-00432-2

Palu, T.; Hall, L.; Edwards, D.; Grosjean, E.; Rollet, N.; Boreham, C.; Buckler, T.; Higgings, K.; Nguyen, D. & Khider, K. 2017. Source Rocks and Hydrocarbon Fluids of the Browse Basin. *In:* AAPG/SEG 2017 International Conference and Exhibition, Oct. 15-18, 2017, London, England. *Search and Discovery Article,* 11028, 9p. https://www.searchanddiscovery.com/pdfz/documents/2017/11028palu/ndx_palu.pdf.html

Peña, K.L. 2022a. Las amenazas del fracking & el manejo de impactos al agua y suelo, por fallamiento y sismicidad inducida. *In:* 4a Jornada Ambiental GEAmbiental, Apr. 22 – 23, 2022, Bucaramanga, Colombia. Presentation 10.

Peña, K.L. 2022b. *Application of the Fracability Index Using Well-logging Data to Evaluate the Sequences BB15 to BB5 in the Browse Basin Northwest Shelf Australia.* Yogyakarta, 219p. Masters Thesis, Postgraduate Program of Geological Engineering, Geological Engineering Department, Universitas Gadjah Mada.

Peña Cerón, K.L.; Surjono, S.S. & Indrawan, I.G.B. 2023. Estimation of Rock Mechanical Parameters Using Well Log Data in the Poseidon 1 Well, Lower Cretaceous, Browse Basin, Northwest Shelf, Australia. *In:* Geoscience and Environmental Management, 3: International Conference of Science and Technology – Universitas Gadjah Mada, 8, Sep. 2022. *IOP Conference Series: Earth and Environmental Science*, Bristol, v. 1233, paper id. 012026, 13p. DOI 10.1088/1755-1315/1233/1/012026

Raymond, O.L.; Totterdell, J.M.; Woods, M.A. & Stewart, A.J. 2018. *Australian Geological Provinces 2018.01 edition*. Canberra, Geoscience Australia, scale 1:1,000,000. https://doi.org/10.26186/116823

Ribeiro, P.; Melo, M. & Nelson, P. 2016. Correlation Between Uniaxial Compressive Strength and Brazilian Tensile Strength Using Different Rock Types. *In:* ISRM VII Brazilian Symposium on Rock Mechanics - SBMR 2016, Belo Horizonte, Minas Gerais, Brazil, Oct. 19–26, 2016. *ISRM VII Bra. Symp. on Rock Mech,* Belo Horizonte, paper number ISRM-SBMR-2016-01. Available in: < https://onepetro.org/ISRMSBMR/proceedings-abstract/SBMR16/All-SBMR16/ISRM-SBMR-2016-01/169835 >. Accessed in: Dec. 2021.

R Foundation for Statistical Computing. 2022. *R*. Vienna, Austria, v. 4.2.0. Available in: < https://www.R-project.org/ >. Accessed in: May. 2022.

Rickman, R.; Mullen, M.; Petre, E.; Grieser, B. & Kundert, D. 2008. A Practical Use of Shale Petrophysics for Stimulation Design Optimization: All Shale Plays Are Not Clones of the Barnett Shale. *In:* SPE Annual Technical Conference and Exhibition, Sep. 2008, Denver, Colorado, USA. *SPE Annu. Tech. Conf. Exhib.,* Denver, Paper Number: SPE-115258-MS. https://doi.org/10.2118/115258-MS

Rollet, N.; Edwards, D.; Grosjean, E.; Palau, T.; Hall, L.; Totterdell, J.; Boreham, C. & Murray, A. 2018. Regional Jurassic sediment depositional architecture, Browse Basin: Implications for petroleum systems. *In:* Australasian Exploration Geoscience Conference, 1st, 2018, Sydney, Australia. *ASEG Extended Abstracts, 2018* (1): 1-8. https://doi.org/10.1071/ASEG2018abM1_3B

Wright, B. 2012. *Unconventionals' Role as a Bridge to the Future*. Available in: < https://jpt.spe.org/unconventionals-role-as-a-bridge-to-the-future >. Accessed in: Oct. 2022.

Zhang, D.; Ranjith, P. & Perera, M. 2016. The brittleness indices used in rock mechanics and their application in shale hydraulic fracturing: A review. *J. Pet. Sci. Eng.*, 143: 158-170. https://doi.org/10.1016/j.petrol.2016.02.011

Zoback, M.D. & Kohli, A. 2019. *Unconventional Resources Geomechanics: Shale Gas, Tight gas, and induced seismicity*. Cambridge, Cambridge University Press, 492p. https://doi.org/10.1017/9781316091869

Zou, C. 2017. *Unconventional Petroleum Geology*. 2nd ed. Elsevier, 500p.